Effect of Thickness and Temperature Variations on Some Structural, Optical and Electrical Properties of Electron Beam Deposited CdS Thin Films

Achiri Celestine Tange[*]

College of Technology, University of Buea, P.O. Box 63 Buea, SW Region, Cameroon

Email: achiri.celestine@ubuea.cm

Abstract

Thin films of cadmium sulfide (CdS) by electron beam deposition on glass substrate. The structure of the films was investigated by X-ray diffraction (XRD). The CdS films were found to be crystalline and hexagonal with the *c*-axis perpendicular to the substrate. Annealing in air at 400^0C greatly improved the crystallinity of the films as well as increasing their grain size. The optical properties of the films have been studied by transmission/reflection spectroscopy. The CdS films had optical bandgaps in the range 2.35-2.42 eV, which were dependent on the film thickness as well as on temperature. A reduction in the bandgap was also noticed for the annealed films. In addition, the single-effective oscillator parameters have been evaluated and their dependence upon film thickness discussed.

From d.c. electrical conductivity measurements it was found that the conductivity of the CdS films is a function of the thickness of the film, increasing with the thicker films. The electrical conductivity is greatly improved when the film is air-annealed. From values of the activation energy of conduction it was concluded that conduction is dominated by states close to the conduction band.

Keywords: II-VI thin films; CdS; electron beam deposition; activation energy; absorption coefficient; optical spectra; optical bandgap; electrical properties.

* Corresponding author.

1. Introduction

Cadmium sulfide belongs to the family of compounds generally referred to as II-VI compound semiconductors [1]. These include the oxides, sulfides, selenides, and tellurides of beryllium, cadmium, magnesium, mercury, and zinc. The compound semiconductors such as cadmium sulphide (CdS), zinc telluride (ZnTe), zinc selenide (ZnSe) are large band gap materials that have found applications in Light emitting diodes (LED)[2], photo catalysis[3,4], detectors and photovoltaics[2,3,5]. Efficient thin films based photonic devices can be fabricated by employing a host of thin film fabrication technologies. Many different techniques have been reported for the preparation of stoichiometric thin films of II-VI compounds among which thermal evaporation [8,14], chemical bath deposition[9,15],pulsed laser deposition[10], electrodeposition[12] and spray pyrolysis[16] are the most commonly used. Cadmium sulfide is a direct band gap n-type semiconductor with a band gap of $E_g = 2.42eV$ [4,6]. It is commonly used as window layer material in CdTe based solar cells [13]. The properties of thin films are greatly affected by their composition and the method of preparation. Thus, thin films prepared by different techniques might show some changes in their structural, optical and electrical properties. Here we present the effect of thickness on the structural, optical and electrical properties of electron beam deposited CdS thin films. The structures of the as-deposited as well as annealed films were studied by X-ray diffraction with Cu k-α line at a wavelength of 1.5418 Å. The optical properties including refractive index, absorption coefficient, and energy band gap were studied by spectrophotometers in the range 200-2500 nm. The electrical properties such as conductivity and resistivity were studied by a four point probe technique.

2. Experimental

The coating system used in the present work is the Edwards E306A high vacuum coating unit equipped with a six position electron beam source, a high vacuum pumping system, digital film thickness monitor and an electromagnetic source shutter. The films were deposited on glass substrate (normal laboratory glass slides, which were cleaned ultrasonically), at a rate of approximately 5 nm / min under a high vacuum (2×10^{-5} torr) and the thickness controlled with the digital film thickness monitor. Automatic termination of deposition is ensured at the specified thickness by remote shutter operation. The CdS films were later air-annealed in a furnace at 400^0C for 2 hrs. The X-ray analyses were performed at room temperature using the Philips PW1710 diffractometer, which is equipped with a curved graphite crystal monochromator. The measurements were performed in the range $2\theta = 2°$ to $2\theta = 120°$ with copper target and nickel filter at 40 kV and 30 mA with a scanning speed of 0.06°/min and incident wavelength λKα = 1.5418 Å. The indexing of the samples was done by using the computer program "Dicvol 91" while average grain size was evaluated from the full width at half maximum (FWHM) of the most intense peaks using Scherrer formula [17].

$$GS = \frac{K\lambda}{\beta \cos\theta} \qquad (1)$$

where *K* is the Scherrer constant (general taken as unity in most cases), β is the FWHM, λ the wavelength of the X-rays and θ the Bragg angle.

The optical transmittance and reflectance were measured using the JASCO V-570 double beam spectrophotometer at normal incidence in the range 200nm-2500nm. The JASCO V-570 instrument, with a resolution of 0.5 nm has a dual detector/grating design and incorporates a photomultiplier detector for UV/ VIS and a PbS photocell detector for NIR regions. This model comes as a stand-alone or fully PC-controlled unit.

All electrical measurements were carried out at room temperature (RT) using a Four-point probe technique to study the electrical behaviour of as-deposited CdS thin films fabricated by electron beam deposition method. The materials used for the deposition of the thin films were bulk single crystals of CdS (99.99%). The chemical composition of the films was verified by X-ray fluorescence spectroscopy (XRF). The relative amount of cadmium in the CdS films was estimated from the intensity of the Cd peaks.

3. Results and Discussion

3.1 Structural

Figure 1 shows the XRD of bulk CdS and as-deposited film of thickness 940nm. This revealed that CdS was the dominant phase in the as-deposited films. The as-deposited films were found to be crystalline with a (002) preferential orientation as can be seen from the single intense peak at $2\theta = 26.5^0$. Comparing the diffraction data with ICDD data card (number 80-0006) revealed that the films possessed the wurtzite hexagonal symmetry.
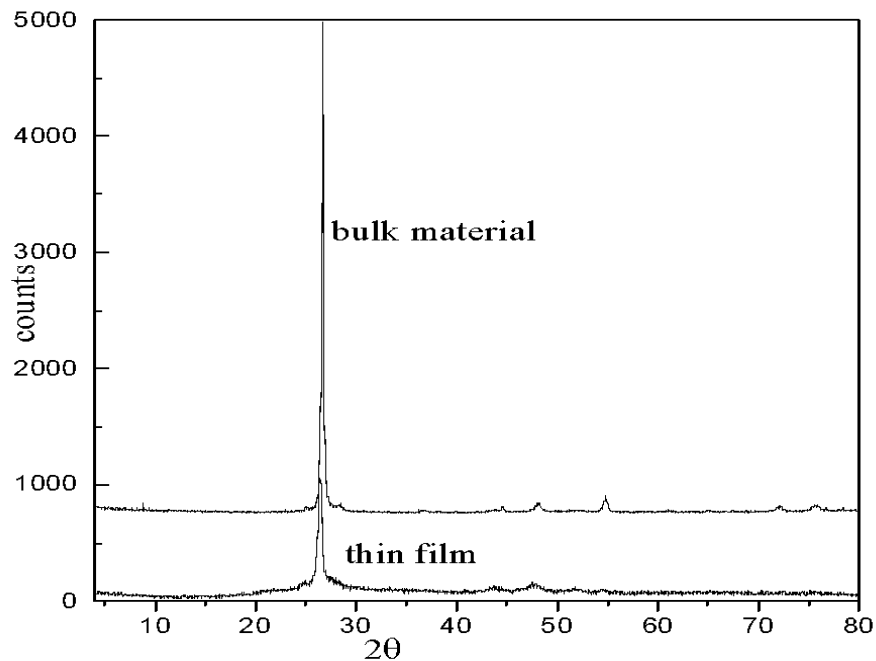

Figure 1: XRD of bulk CdS and as-deposited film of thickness 940nm.

Peak broadening has been used to indicate crystallinity (grain size), relative intensities were used to indicate texture and peak positions were used to determine lattice parameters. From the Scherrer formula the grain size of the crystallites was found to increase with increasing film thickness (see Fig.2 and Table 1), which is evidenced from the broadening of the (002) peak. From the relative intensities of the (002) we observed that there is a significant change in film grain texture as the film thickness increases, as indicated by the gross change in relative intensities. Before performing any analysis using the X-ray scan the background due to the glass substrate was subtracted, so as to get a clear picture of the peak broadening.
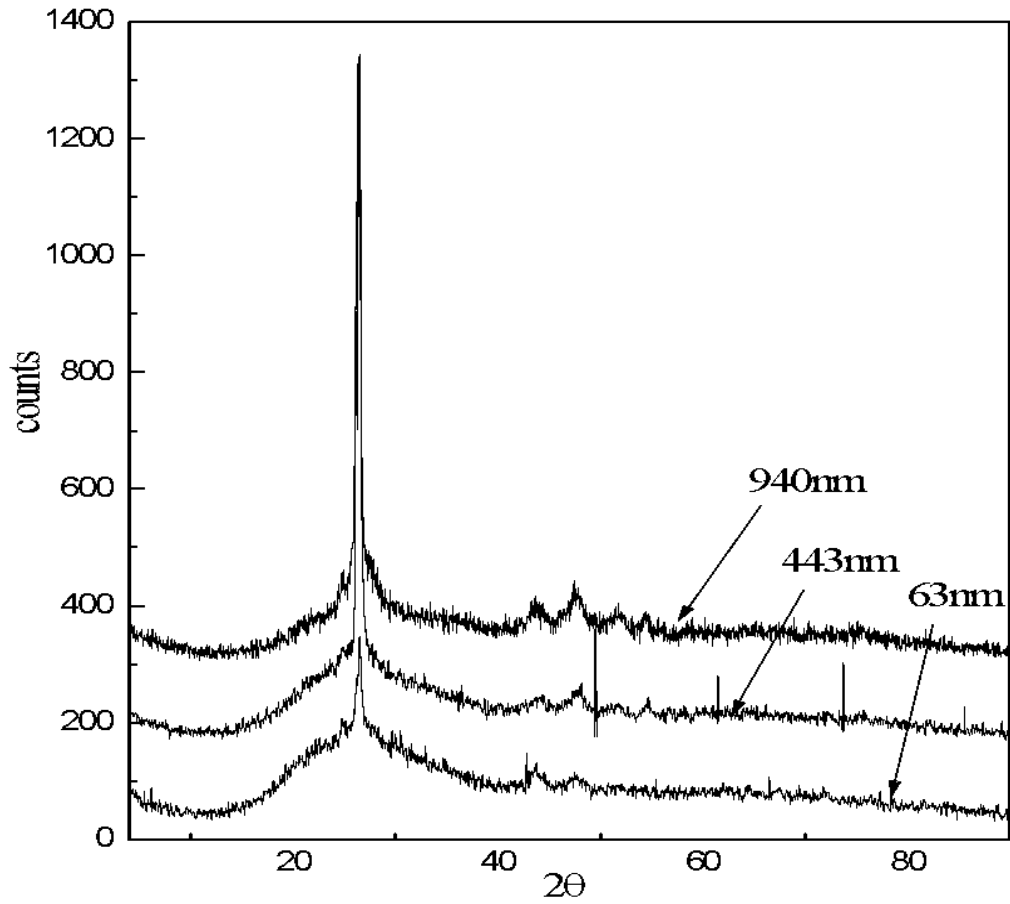
Figure 2: XRD of films of different thicknesses clearly showing the change in texture and the effect of the glass substrate as film thickness increases.

The annealed films still had CdS as the dominant phase. There was a general improvement in the film crystallinity as well as an increase in the grain size after annealing. Since thicker films have bigger crystallites they are closer to the crystalline CdS, but bigger grain sizes results in larger unfilled inter-granular volume so that the absorption per unit thickness is reduced. Thus we would expect the thicker films to have smaller bandgaps.
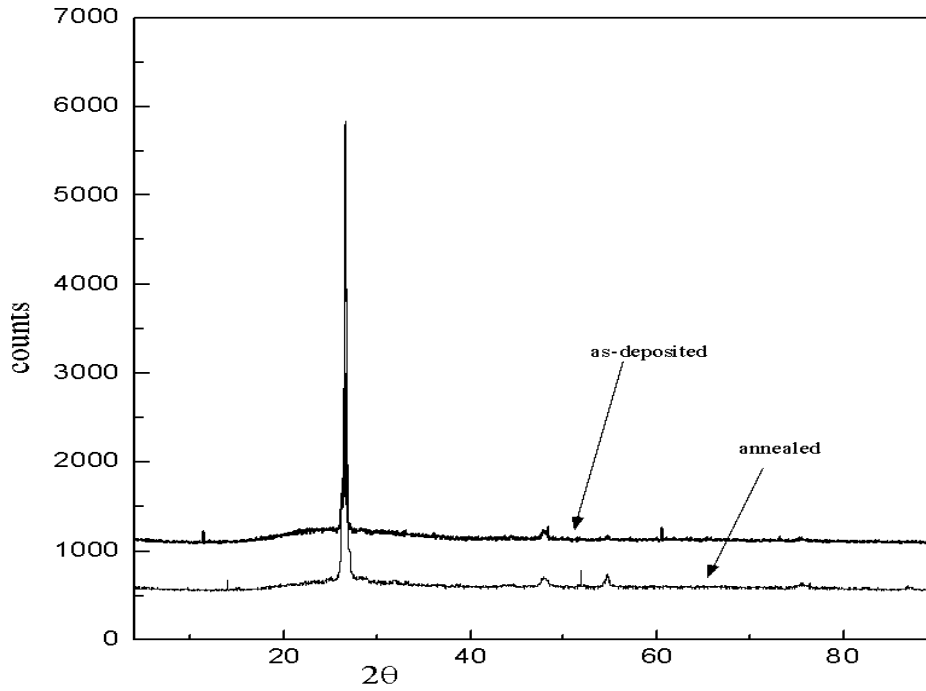
Figure 3: XRD of as-deposited and annealed films of thickness 940nm.

Table 1: Calculated grain sizes for as-deposited and annealed films.

Film Thickness(nm)	Grain size(nm) As-deposited	Annealed
63	18.68	20.07
443	20.38	22.66
940	29.25	45.85

3.2 Optical

The optical parameters, namely, the absorption coefficient (α), extinction coefficient (k) and refractive index (n) have been calculated from the transmittance and reflectance data. The real and imaginary parts of the dielectric constant (ε_1 and ε_2) were computed from *n* and *k*.

$$\widetilde{\varepsilon} = \varepsilon_1 + i\varepsilon_2 \qquad (2)$$

$$\varepsilon_1 = n^2 - k^2 \qquad (3)$$
$$\varepsilon_2 = 2nk$$

In addition, the single-effective oscillator parameters have also been computed. The index of refraction and the dielectric function are highly frequency dependent. This frequency dependency is expressed through the dipole oscillator model [18,19].

$$\varepsilon_1(E) = 1 + \frac{F}{E_0^2 - E^2} \qquad (4)$$

where E_0 is the single oscillator energy and has a direct relation with the electric dipole strength F. By defining $E_d = F/E_0$ (here E_d is a measure of the strength of interband optical transitions in the transparent region) and after eliminating k,

$$(n^2 - 1)^{-1} = \left(-\frac{1}{E_d E_0}\right) E^2 + \frac{E_0}{E_d} \qquad (5)$$

Values of the parameters E_0 and E_d can be obtained by plotting $(n - 1)^{-1}$ against E^2.
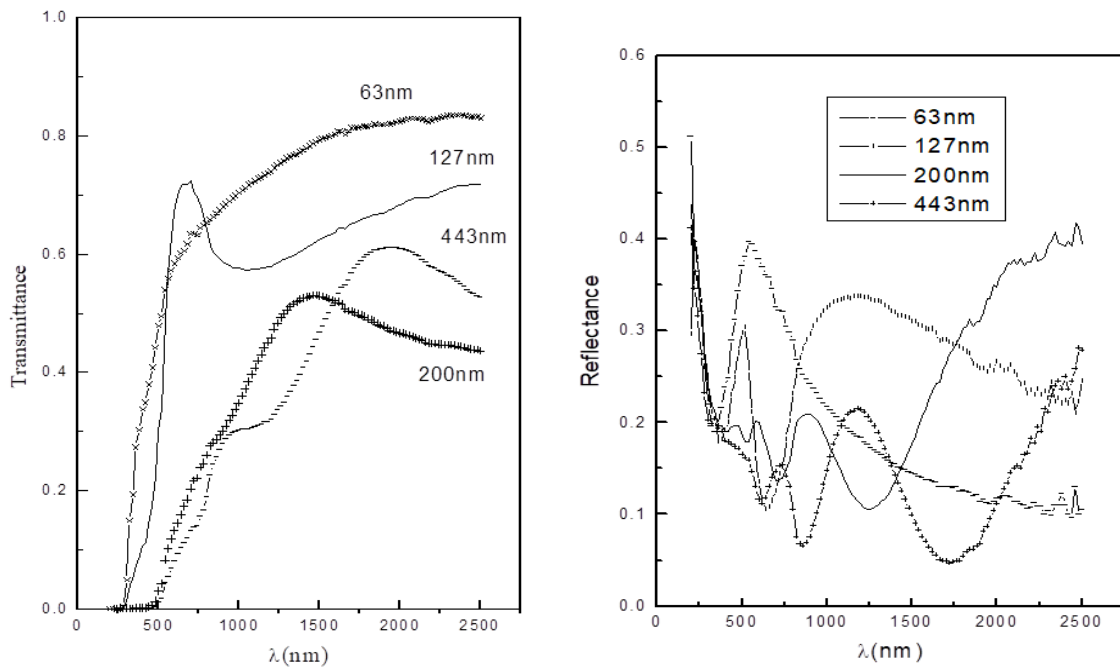

Figure 4: Spectral transmittance and reflectance for films of different thickness.

Figure 4 shows the spectral transmittance and reflectance for films of different thickness. The onset of absorption (absorption edge) shifts towards ~500 nm as the film thickness increases. The films have transmittance in the visible and near infrared regions of about 55-80 %. Such high transmittance for CdS thin films is well suited for this material to be used as window materials in heterojunction solar cells. The oscillations in the reflectance spectra are due to the constructive and destructive interference between the film layers and between the film and the glass substrate.

Figure 5 below shows the variation of refractive index with photon energy *hv* for annealed films of thickness 940 nm. The variation of the refractive index with photon energy tends to follow the dipole oscillator model, clearly showing the dispersion of the refractive index after the annealing process. This variation is seen to

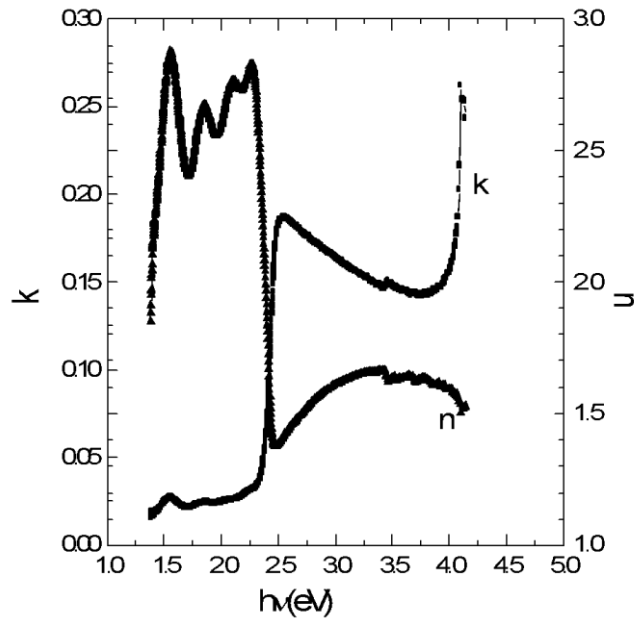increase as the film thickness increases.

Figure 5: Variation of refractive index with photon energy for annealed CdS film of thickness 829nm.
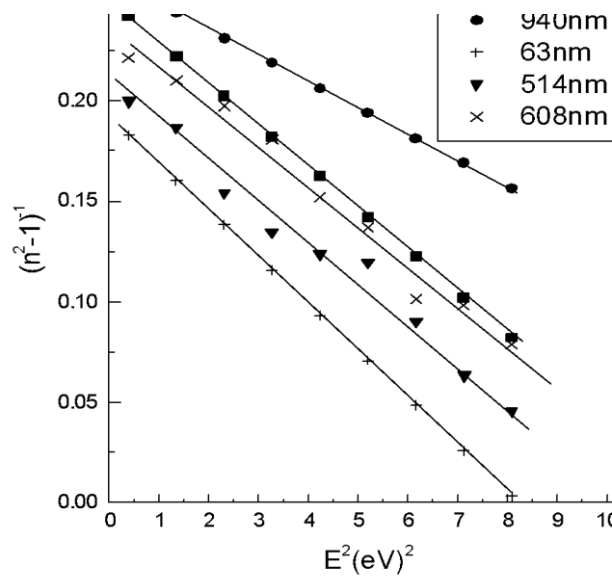

Figure 6: $(n^2-1)^{-1}$ versus E^2 for films of different thickness, d, annealed at 400^0C.

Following the single-effective oscillator model [18,19] values of the single oscillator energy E_0 and the electronic dispersion energy E_d have been evaluated for the films annealed at 400^0C (see Fig. 6 and Table 2). The results show a strong dependence on the film thickness. Both E_d and E_0 are seen to increase with increase in

film thickness, indicating an increase in interband transitions for the thicker films.

Table 2: Single-effective oscillator parameters.

Film Thickness (nm)	63	514	608	829	940
E_d (eV)		14.86	15.213	15.772	15.96	17.22
E_0 (eV)		3.247	3.271	3.314	3.48	4.5

The absorption coefficient α is the parameter that quantifies the absorption of light in a medium. It is defined as the fraction of the power absorbed in a unit volume per unit incident flux of the incident electromagnetic radiation. It has a strong dependence on the frequency of the incident radiation. The absorption coefficient of the films was measured using the well known using Tauc's ratio [20]:

$$\alpha = \frac{-1}{d}\ln(\frac{1}{T}) \quad (6)$$

where d and T are thickness and the transmittance respectively of the CdS thin films shown in Fig. 4. The relationship between the absorption coefficient (α) and the optical bandgap ($\square_\square$) film can be expressed by the following equation

$$\alpha h\upsilon = A(h\upsilon - E_g)^{1/2} \quad (7)$$

where A is a constant. From this dependence we can effectively determine the energy gap by plotting $(\square h\upsilon)^2$ against photon energy $h\upsilon$ and extrapolating the linear part to $(\square h\upsilon)^2 = 0$. The absorption coefficients are in the order of 10^4 cm^{-1}. Plots of $(\alpha h\upsilon)^2$ against $h\upsilon$ have been carried out for both as-deposited (Fig. 7a &7c) and annealed (Fig.7b&7d). The films of thickness 127nm and 200nm are shown as two examples. Extrapolating the linear section of the curve to $(\alpha h\upsilon)^2 = 0$ reveals bandgaps that range between 2.35eV to 2.42eV. The bandgap was found to decrease with increasing film thickness. One could consider this decrease in the bandgap with increasing thickness (grain size) as indicative of a decreasing grain boundary barrier height with increasing grain size. Plots of $(\alpha h\upsilon)^{1/2}$ and $(\alpha h\upsilon)^{3/2}$ against $h\upsilon$ did not show any good linear approximation confirming that the fundamental optical absorption in the CdS films is direct.
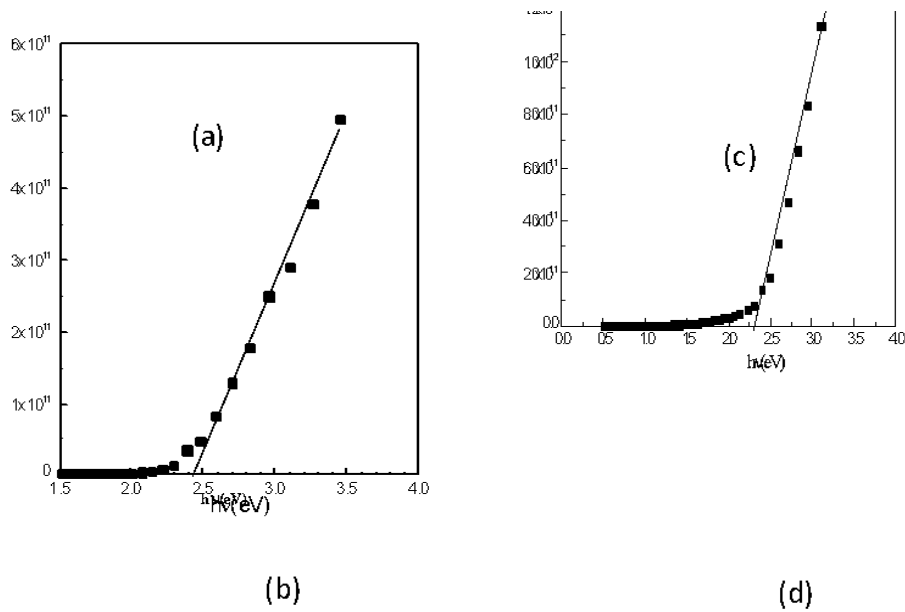
Figure 7: Variation of $(\alpha h\upsilon)^2$ Vs *hυ* for as deposited CdS film of thickness (a)127nm (c) 200nm and annealed (b) 127nm (d) 200nm.

After annealing in air at 400^0C for two hours, a decrease in the bandgap was observed for some of the films. The film of thickness 63nm had bandgap of 2.42 eV and 2.12 eV for the as-deposited and annealed films, respectively whereas the film of thickness 127nm had bandgaps of 2.40 eV and 2.395 eV for the as-deposited and annealed films, respectively. This reduction in the bandgap is probably due to a change in the composition which may have resulted to a shift in the valence band or conduction band. Such shifts are possible in air annealed samples due to the formation of cadmium oxide (CdO) [21]. Our XRD study was unable to detect cadmium oxide, probably because the CdO content was too small to be detected. The films of thickness 200nm and 443nm showed an increase in their bandgap instead; from 2.35 eV to 2.40 eV and 2.42 eV, respectively. Such an increase has also been reported [4,22] for RF sputtered CdS films annealed at 150^0C. Due to the expansion and contraction of the lattice with temperature the various band parameters especially the bandgap is temperature dependent. The effect of temperature change in the range 5-70 ^{0}C on the transmittance has been carried out in order to determine the variation of the optical bandgap with temperature. For the film of thickness 443 nm, it was found that the transmittance decreases with increasing temperature up to 35^0C (Fig. 8). Consequently E_g decreases steadily with temperature but attained a saturation value of 2.43 eV at 35^0C. Studying the variation of E_g with temperature is important in understanding the rapidity of the interband transitions at the band edge.
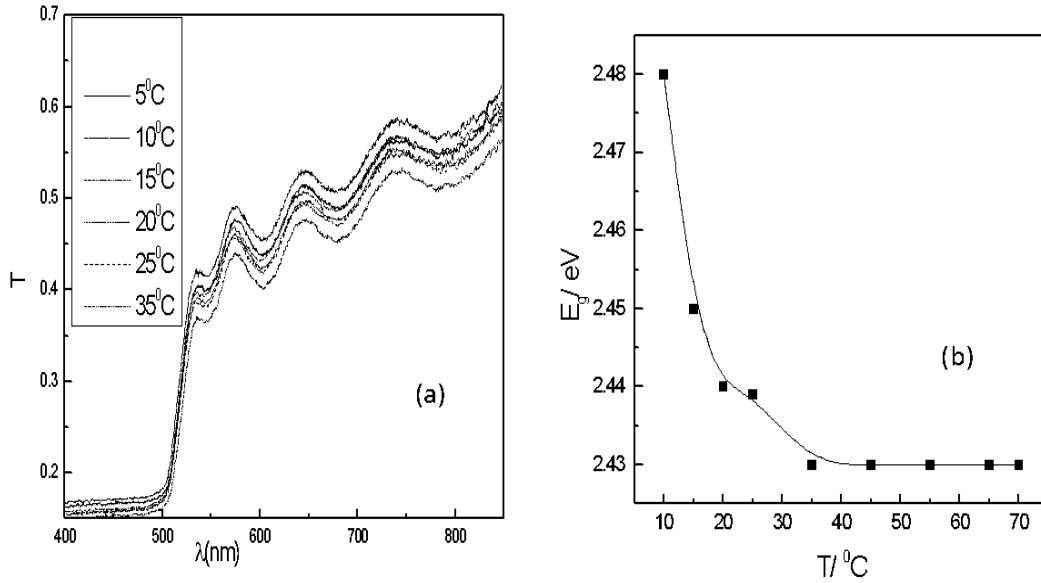
Figure 8: Variation of (a) transmittance (b) E_g with temperature for film of thickness 443nm.

3.3. Electrical properties

Figure 9 below shows the variation of the resistance of as-deposited CdS films with temperature while Figure 10 shows the corresponding Arrhenius plots for films of different thicknesses. The films had high resistance in the range 10^4-10^6 Ω. The results show that the resistance of the films decrease with increasing film thickness.
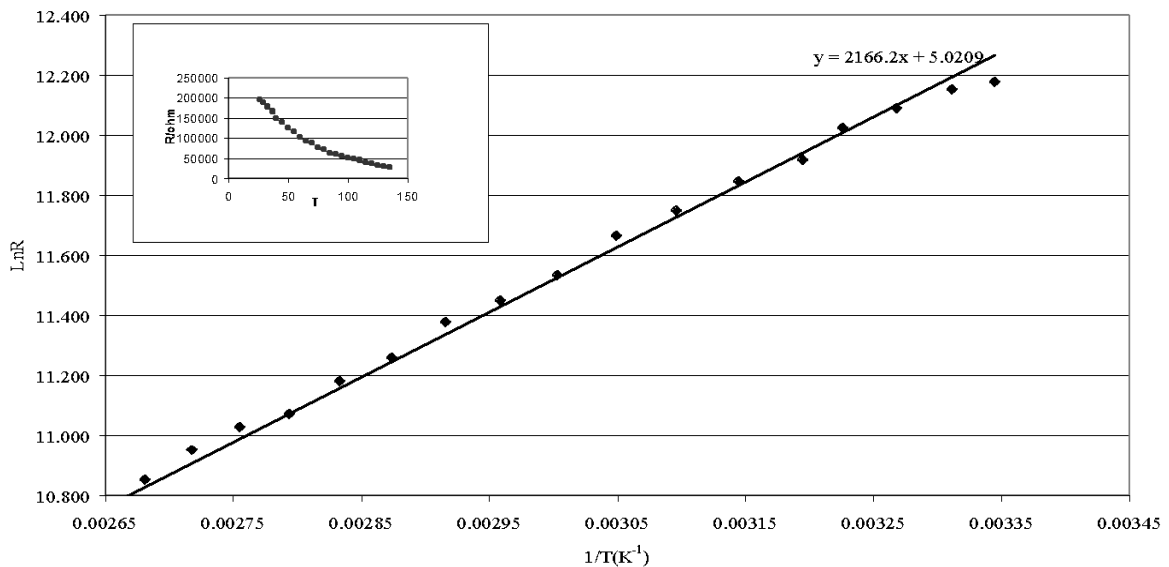

Figure 9: Arrhenius plot for as deposited CdS film of thickness 514nm.The inset shows the variation of R with temperature, clearly showing the semiconducting nature of the film.
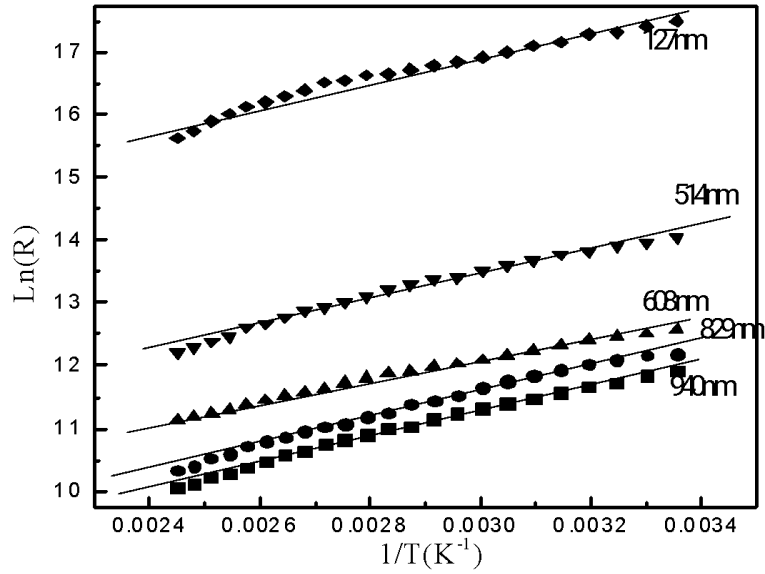
Figure 10: Arrhenius plots for CdS films of different thicknesses.

Since the electrical conductivity is proportional to the product of charge carrier concentration and mobility, the decrease in film resistivity with increase in film thickness has been attributed to an increase of carrier concentration and mobility of the thicker films. The activation energies of conduction have been evaluated from the slopes of the straight line graphs in Figure 10 following the equation

$$R = R_0 \exp\left(\frac{\Delta E}{2kT}\right)$$

(8)

These values of the activation energy (see Table 3) show that the Fermi energy is above the (E_g / 2) level. Consequently the electrical conduction is controlled by states near the conduction band.

Table 3: Activation energy of conduction for CdS films.

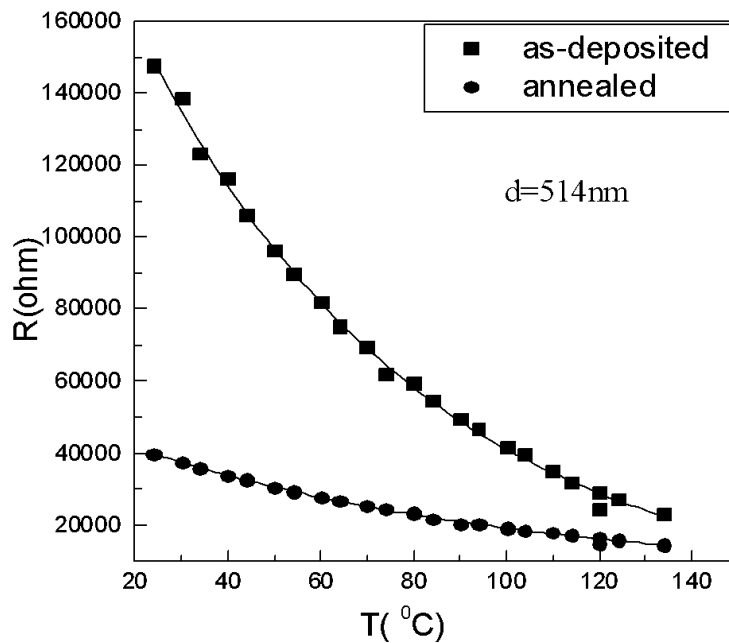| Film Thickness(nm)	127	514	608	829	940
ΔE(eV)	0.38	0.374	0.356	0.356	0.28

Figure 11: Comparison of temperature variation with resistance for as-deposited and annealed films of thickness 514nm.

Figure 11 shows the film resistance versus temperature for as-deposited and annealed CdS film of thickness 514nm. The resistance was found to reduce considerably after annealing. There exist defects such as point defects, impurities, dislocations, etc in as-deposited films. Heat treatment (in this case annealing) can reduce point defects in the films resulting in a decrease in the resistivity. Moreover, the growth in the grain size also contributes in improving the electrical properties. In the present study the decrease in the film resistivity upon annealing has been attributed to a decrease in the point defects, increase in grain size and an overall improvement on the grain lattice integrity of the films. In addition it was observed that the annealing increases the smoothness (reduction in surface roughness) of the films, hence the elimination of islands, thereby causing a decrease in the film resistivity.

4. Conclusion

Thin films of cadmium sulfide have been prepared by the physical vapor technique of electron beam deposition in high vacuum. The structure of the films has been studied by X-ray diffraction; the optical properties were studied using transmission/reflection spectroscopy and the electrical conductivity as a function of temperature has also been studied. XRD analysis showed that the as-deposited CdS films were crystalline with a (002) preferential orientation. The films possessed hexagonal symmetry with the *c*-axis perpendicular to the substrate. The crystallinity of the films was found to increase with increasing film thickness. The calculated grain sizes also followed this trend. After annealing in air at 400^0C for two hours, the crystallinity of the films was improved as well as an increase in their grain size noticed. The optical parameters, namely, refractive index, extinction coefficient and absorption coefficient have been computed from the transmittance/reflectance data

and results compared for as-deposited and air-annealed samples. The optical bandgaps have also been evaluated and their variation with thickness and temperature studied. In addition, the single-effective oscillator parameters have been evaluated for the CdS films and their variation with film thickness studied. For the CdS films the bandgap was found to decrease with increasing film thickness, a fact attributed to decreasing grain boundary barrier height with increasing grain size. In addition, the decrease in bandgap after annealing was attributed to compositional changes. The as-deposited CdS films had high specific resistance that was considerably reduced when the films were air-annealed. This reduction in the resistance was attributed to a reduction in the point defects and roughness of the films after annealing. Values of the activation energy of conduction were evaluated and it was observed that the conduction was dominated by states close to the conduction band. These results show that thin films of CdS can effectively be produced by electron beam deposition with good optical and electrical properties that can be improved by heat treatment. Such films can be used as good window materials for heterojunction solar cells.

Acknowledgements

References

[1] Brian Ray, *II-VI Compounds*, International Series of Monographs in the Science of the Solid State Vol.2 (1969)

[2] A.S. Lahewil, Y. Al-Douri, U. Hashim, N.M. Ahmed, *Structural and optical investigations of cadmium sulfide nanostructures for optoelectronic applications,* Solar Energy, 86(11), 3234 (2012)

[3] N. Amin, K. Sopian, M. Konagai, Sol. Energy Mater. Sol. Cells, 91(13), 1202(2007)

[4] Kumar S, Sharma P, Sharma V. *CdS nanofilms: Synthesis and the role of annealing on structural and optical properties*. J Appl Phys. 2012;111(4)

[5] Tsai K-A, Hsu Y-J. *Graphene quantum dots mediated charge transfer of CdSe nanocrystals for enhancing photoelectrochemical hydrogen production*. Appl Catal B Environ. 2015

[6] Spirito D, Kudera S, Miseikis V, Giansante C, Coletti C, Krahne R. *UV Light Detection from CdS Nanocrystal Sensitized Graphene Photodetectors at kHz Frequencies.* J Phys Chem C. 2015;119(42):23859-23864.

[7] Bao Z, Liu L, Yang X, et al. *Synthesis and characterization of novel oxygenated CdSe window layer for CdTe thin film solar cells.* Mater Sci Semicond Process. 2017;63:12-17

[8] Shah NA, Mahmood W. Physical properties of sublimated zinc telluride thin films for solar cell applications. *Thin Solid Films*. 2013;544:307-312.

[9] Hegde SS, Kunjomana AG, Prashantha M, Kumar C, Ramesh K. *Photovoltaic structures using thermally evaporated SnS and CdS thin films.* Thin Solid Films. 2013;545:543-547

[10] Kumar P, Saxena N, Gupta V, Gao K, Singh F, Agarwal A. *Effect of swift heavy ions on pulsed laser deposited Ag doped CdS nanocrystalline thin films.* Adv Sci Lett. 2014;20(5- 6):977-983

[11] Ferrá-González SR, Berman-Mendoza D, García-Gutiérrez R, et al. *Optical and structural properties of CdS thin films grown by chemical bath deposition doped with Ag by ion exchange*. Opt - Int J Light Electron Opt. 2014;125(4):1533-1536

[12] K. Sheshan, *Handbook of Thin Film Deposition Processes and Techniques*, William Andrew Publishing/Noyes (2002)

[13] Mahmood W, Shah NA. *Study of cadmium sulfide thin films as a window layers*. AIP Conf Proc. 2012;1476:178-182

[14] Tariq GH, Anis-ur-Rehman M. *Characterization of Physical Properties of Thermally Evaporated Doped CdS Thin Films for Photovoltaics.* Key Eng Mater. 2012;510-511:156- 162

[15] Moualkia H, Hariech S, Aida MS. *Structural and optical properties of CdS thin films grown by chemical bath deposition.* Thin Solid Films. 2009;518(4):1259-1262.

[16] Aksay S, Polat M, Özer T, Köse S, Gürbüz G. *Investigations on structural, vibrational, morphological and optical properties of CdS and CdS/Co films by ultrasonic spray pyrolysis*. Appl Surf Sci. 2011;257(23):10072-10077

[17] Cullity, B.D., *Elements of X-ray Diffraction,* Prentice Hall 2001 (3rd edition)

[18] Max Fox , *Optical Properties of Solids*, Oxford Master Series in Condensed Matter Physics, OUP (2001)

[19] S.H. Wemple, M. Di Domenico, Phys. Rev. B, **3** 1338 (1971)

[20] J. Tauc (ed) *Amorphous and liquid semiconductors*. (Springer, Berlin, 2012).

[21] S. Mahanty, D. Basak, F. Rueda, M. Leon, *Journal of Electronic Materials,* **28** (5), 559-562 (1999)

[22] K. El Assali, M. Boustani, A. Khiara, T. Bekkay, A. Outzourhit, E.L. Ameziane, J.C. Bernede, J. Pouzet, Physica Status Solidi, **178** (2) pp. 701-708 (2001)